

# Plasma Wakefield Acceleration with a Modulated Proton Bunch

A. Caldwell

*Max-Planck-Institut für Physik, 80805, München, Germany*

K. V. Lotov

*Budker Institute of Nuclear Physics, 630090, Novosibirsk, Russia*

*Novosibirsk State University, 630090, Novosibirsk, Russia*

(Dated: August 23, 2018)

The plasma wakefield amplitudes which could be achieved via the modulation of a long proton bunch are investigated. We find that in the limit of long bunches compared to the plasma wavelength, the strength of the accelerating fields is directly proportional to the number of particles in the drive bunch and inversely proportional to the square of the transverse bunch size. The scaling laws were tested and verified in detailed simulations using parameters of existing proton accelerators, and large electric fields were achieved, reaching 1 GV/m for LHC bunches. Energy gains for test electrons beyond 6 TeV were found in this case.

PACS numbers: 41.75.Lx, 52.35.Qz, 52.40.Mj

Proton-driven plasma-wakefield acceleration has been proposed recently as a means of accelerating bunches of electrons to high energies [1, 2]. The basic idea is to use a plasma to transfer the energy from a bunch of protons, which can be accelerated to the multi-TeV regime today in existing accelerators, to a bunch of electrons, for which energies have so far been limited to about 100 GeV due to synchrotron radiation losses in circular accelerators. In [1, 2], the proton bunch was assumed to have been compressed to an rms length of 100  $\mu\text{m}$  to achieve the strong accelerating fields in the plasma. Such short proton bunches are not available today, and compression schemes, while conceivable [3, 4], will require long distances and substantial RF power, and will therefore be costly. A possible alternative to bunch compression is to start with an existing long proton bunch and divide it up into a series of microbunches in a plasma. A long proton bunch propagating in a plasma will naturally be modulated at the plasma wavelength, and the modulated bunch will in turn set up oscillations of the plasma electrons. The modulation of the bunch grows rapidly from noise and the growth rate has recently been studied theoretically [5], with calculations showing that the modulation can be very effectively produced.

We report here both parametric studies and simulation results for the electric fields which can be achieved via this mechanism, and discuss achievable energy gains using CERN PS, SPS and LHC bunch parameters as concrete examples. We start with a brief review of the relevant formulae for the axial electric fields produced by bunches of charged particles in a plasma in the linear regime. This is followed by a discussion on the conditions necessary to reach the regime of strong modulations, and simulation results are shown depicting this growth of modulations. We then discuss the conditions necessary for reaching maximum accelerating fields, and show comparisons of our calculations with simulations. Finally, we discuss the limitations on energy gain for bunches of electrons and summarize the results for dif-

ferent driving bunch parameters.

## I. SINGLE BUNCH

For Gaussian shaped drive bunches in the linear regime (where the bunch charge density is much lower than the plasma electron density), the maximum axial electric field is given by [6]

$$\begin{aligned} E_{z,\text{max}} &= eNk_p^2 \exp\left(-\frac{k_p^2\sigma_z^2}{2} + \frac{k_p^2\sigma_r^2}{2}\right) \Gamma(0, k_p^2\sigma_r^2/2) \\ &= eNZ(k_p, \sigma_z)R(k_p\sigma_r) \end{aligned} \quad (1)$$

with

$$Z(k_p, \sigma_z) = k_p^2 \exp\left(-\frac{k_p^2\sigma_z^2}{2}\right), \quad (2)$$

$$R(k_p\sigma_r) = \exp\left(\frac{k_p^2\sigma_r^2}{2}\right) \Gamma(0, k_p^2\sigma_r^2/2), \quad (3)$$

where  $\Gamma(\alpha, \beta) = \int_{\beta}^{\infty} t^{\alpha-1} e^{-t} dt$  is the incomplete Gamma function,  $e$  is the fundamental electric charge,  $N$  is the number of particles in the driving bunch,  $\sigma_z$  is the rms length of the driving bunch,  $\sigma_r$  is the rms transverse size of the driving bunch in one dimension (two transverse sizes are assumed equal), and  $k_p = \omega_p/c$  is the plasma wavenumber determined by the plasma frequency  $\omega_p$  and the driver velocity that is close to the light velocity  $c$ . For a fixed bunch length  $\sigma_z$ , the maximum of  $Z$  is given by  $k_p^2\sigma_z^2 = 2$ . In our considerations (modulation of a long bunch),  $\sigma_z$  for a microbunch is completely fixed by  $k_p$  in such a way that that this condition is approximately satisfied.

The function  $R(k_p\sigma_r)$  peaks at small  $k_p\sigma_r$  and can be parametrized for  $0.04 < k_p\sigma_r < 1.3$  to better than 10 %

accuracy as

$$R(k_p\sigma_r) \approx \frac{7.2 \exp(-k_p\sigma_r/5)}{1 + 5k_p\sigma_r}.$$

We see from these formulae that small transverse sizes of the proton bunch are critical, as well as maximum plasma density. We determine the optimum conditions below.

## II. MODULATED BUNCH

Suppose we have  $\sigma_{z,0}k_p \gg 1$ , where  $\sigma_{z,0}$  is the initial length of the proton bunch as it enters the plasma. Under the right conditions, an instability will be quickly amplified resulting in microbunching of the long bunch. The number of e-foldings of the initial instability scales [5] as

$$N_e \approx 0.3 \xi^{2/3} \tau^{1/3} \quad (4)$$

where  $\xi$  is the distance along the bunch in the co-moving frame in units of  $k_p^{-1}$  and  $\tau$  is the ‘time’ the bunch has traveled in the plasma in units  $c/\omega_b$ . Here

$$\omega_b = \sqrt{\frac{4\pi n_b e^2}{\gamma_b M}},$$

$M$  and  $\gamma_b$  are the mass and relativistic factor of the driving bunch particles, and  $n_b$  is the typical bunch density that, in the central part of the Gaussian bunch, is

$$n_b = \frac{N}{(2\pi)^{3/2} \sigma_r^2 \sigma_z}. \quad (5)$$

Note that this definition of  $\tau$  differs from that in [5] by the factor of  $\sqrt{2}$ .

Table I gives the value of  $c/\omega_b$  taking the peak density for PS, SPS and LHC bunch options. Expression (4) is applicable if  $\tau$  is much greater than the e-folding time, which is not strictly applicable to our case, but the regime characterized by (4) is the one we want to reach. As seen from the table, we will need a very long plasma cell to reach large values of  $\tau$ .

We would like to have a well developed modulation in the center of the bunch, since this is where the bulk of the protons reside. Assuming  $\tau$  will be a number of order 1, we need to have large values of  $\xi$  to make sure the modulation is well developed. This implies that the plasma wavelength should be much shorter than the bunch length. Indeed, we would want to maximize  $k_p\sigma_{z,0}$ . However, we need the plasma skin depth to be at least as large as the transverse size of the bunch, i.e.,

$$\frac{c}{\omega_p} \geq \sigma_r$$

or

$$k_p\sigma_r \leq 1.$$

TABLE I: PS, SPS and LHC parameter sets. The different symbols are defined in the text. SPS-LHC means the standard parameters of bunches in the SPS for injection into the LHC. SPS-Totem means the special parameters for bunches for use by the Totem experiment.

Parameter	PS	SPS-LHC	SPS-Totem	LHC
$W_P$ (GeV)	24	450	450	7000
$N_P$ ( $10^{10}$ )	13	11.5	3.0	11.5
$\sigma_P$ (MeV)	12	135	80	700
$\sigma_{z,0}$ (cm)	20	12	8	7.6
$\sigma_r$ ( $\mu\text{m}$ )	400	200	100	100
$c/\omega_b$ (m)	2.3	4.0	3.2	6.3
$\sigma_\theta$ (mrad)	0.25	0.04	0.02	0.005
$L_\theta$ (m)	1.6	5	5	20
$\epsilon$ (mm-mrad)	0.1	0.008	0.002	$5 \cdot 10^{-4}$

If this requirement is not imposed, filamentation of the bunch could likely develop instead of the axisymmetric instability mode. For a fixed value of  $\sigma_r$ , examination of the formulae in the previous section indicate that the optimum fields under this requirement will be achieved for  $k_p\sigma_r = 1$ , and we will use this in the following calculations. The plasma frequency  $\omega_p$  is related to the plasma density  $n_p$  as

$$\omega_p = \sqrt{\frac{4\pi n_p e^2}{m}},$$

where  $m$  is the electron mass. Fixing  $k_p\sigma_r = 1$  implies that the plasma density is fixed once we fix the transverse size of the proton bunch, as are the frequency  $\omega_p$  and wavelength  $\lambda_p$  of the plasma oscillations. A useful relation is

$$\lambda_p \approx 1 \text{ mm} \sqrt{\frac{10^{15} \text{ cm}^{-3}}{n_p}}.$$

The values for the optimal density and plasma wavelength are given in Table II for the different bunch parameters. The typical plasma densities of interest will be around  $10^{15} \text{ cm}^{-3}$  and the resulting plasma wavelengths around 1 mm.

Since the upper limit on  $k_p$  is fixed from the bunch radius, it is seen that maximizing  $\xi$  implies maximizing the aspect ratio of the bunch  $\sigma_{z,0}/\sigma_r$ . In practice, there will be a limit to the number of microbunches which will behave in a coherent manner due to phase slippage of the instability relative to the bunch, plasma density variations, etc. However, the proton bunch should have a very large aspect ratio in order to reach the stage of strong modulation. This is the case for existing proton bunches, including those listed in Table I.

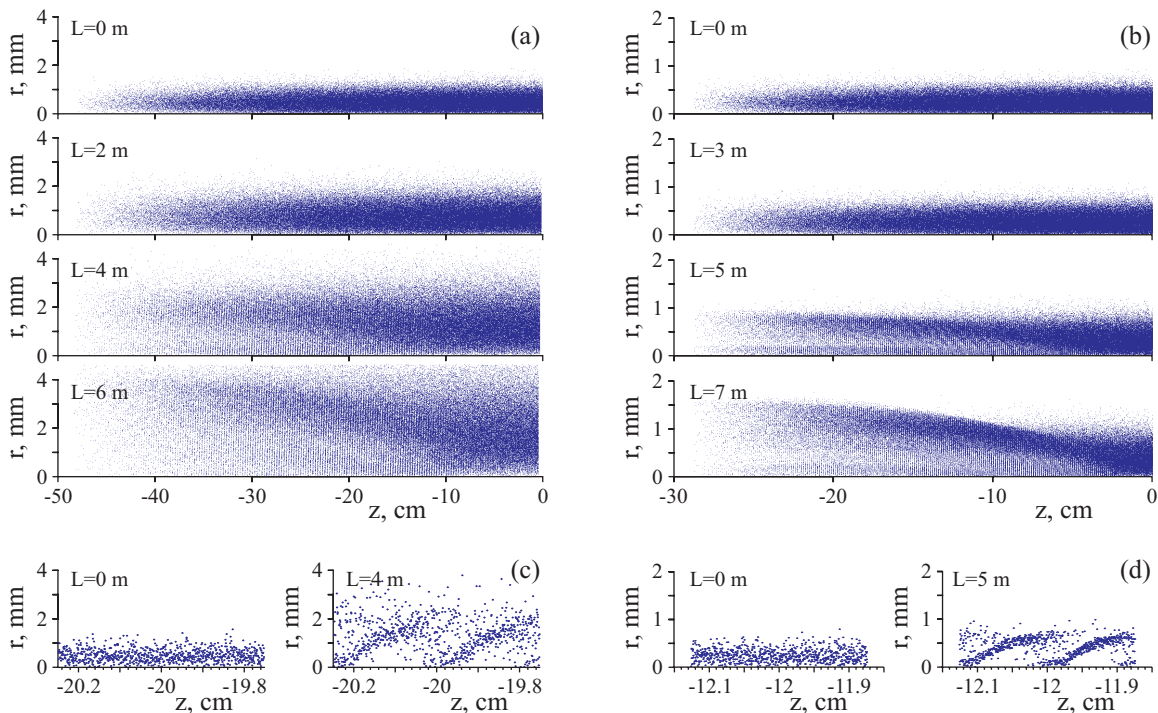


FIG. 1: (Color online) Bunch portraits at different propagation lengths showing the part of the bunch traveling in the plasma (a,b) and the zoomed area located  $\approx \sigma_z$  behind the bunch center (c,d) for the PS bunch (left) and SPS-LHC bunch (right).

TABLE II: Optimal values for the plasma density and resulting values of the parameters defined in the text.

Parameter	PS	SPS-LHC	SPS-Totem	LHC
$n_p$ ( $10^{15} \text{ cm}^{-3}$ )	0.18	0.7	3.0	3.0
$\lambda_p$ (mm)	2.5	1.3	0.6	0.6
$W_f$ (eV)	180	280	100	410
$W_{tr}$ (eV)	750	360	90	90
$eE_{z,\max}$ (GeV/m)	0.1	0.35	0.35	1.4
$eE_0$ (GeV/m)	1.3	2.5	5.3	5.3
$\alpha$	0.08	0.15	0.07	0.25

### III. SIMULATION RESULTS FOR INSTABILITY DEVELOPMENT

The development of the modulation has been studied in simulations using both a seeded and unseeded instability. Only results for the seeded case are reported here. Somewhat higher gradients were observed in simulations for the unseeded case, but we believe the results for the seeded instability are more reliable.

The proton bunch was simulated with a cosine profile given by

$$n_P = \frac{N_P}{2\sigma_r^2\sigma_z(2\pi)^{3/2}} e^{-r^2/2\sigma_r^2} \left[ 1 + \cos\left(\sqrt{\frac{\pi}{2}} \frac{z}{\sigma_z}\right) \right]$$

with the limit  $|z| < \sigma_z\sqrt{2\pi}$ . For the seeded case, it was assumed the plasma was created simultaneously with the passage of the proton bunch, and started at the midpoint of the bunch (e.g., via a co-propagating laser pulse [7]). We used the 2D axisymmetric code LCODE with the fluid model for plasma electrons [8, 9]. Since the beam-to-plasma density ratio is less than 0.3% for all considered variants, the plasma wave does not break and can be safely described within the fluid approximation.

Figure 1 shows the development of the seeded instability for PS and SPS-LHC bunches. Only the parts of the bunch propagating in the plasma are shown. In both cases we observe strong modulation of the bunch density and the typical trumpet-like structure of the disrupted bunch after several meters of propagation. There is, however, a qualitative difference between these two cases, which is more visible in Figure 2. While the SPS-LHC bunch widens due to the instability, the divergence of the PS bunch is caused mainly by the angular spread of the beam particles. In the latter case, the instability develops against the background of this divergence and produces much lower fields as a result.

We consider bunch divergence more closely. The angular spread  $\sigma_\theta$  of the bunch is related to its radius  $\sigma_r$  via the emittance  $\epsilon$ :

$$\sigma_\theta = \epsilon/\sigma_r.$$

The distance at which a particle shifts transversely by the distance of about  $\sigma_r$  is  $L_\theta = \sigma_r/\sigma_\theta = \sigma_r^2/\epsilon$ ; that is,

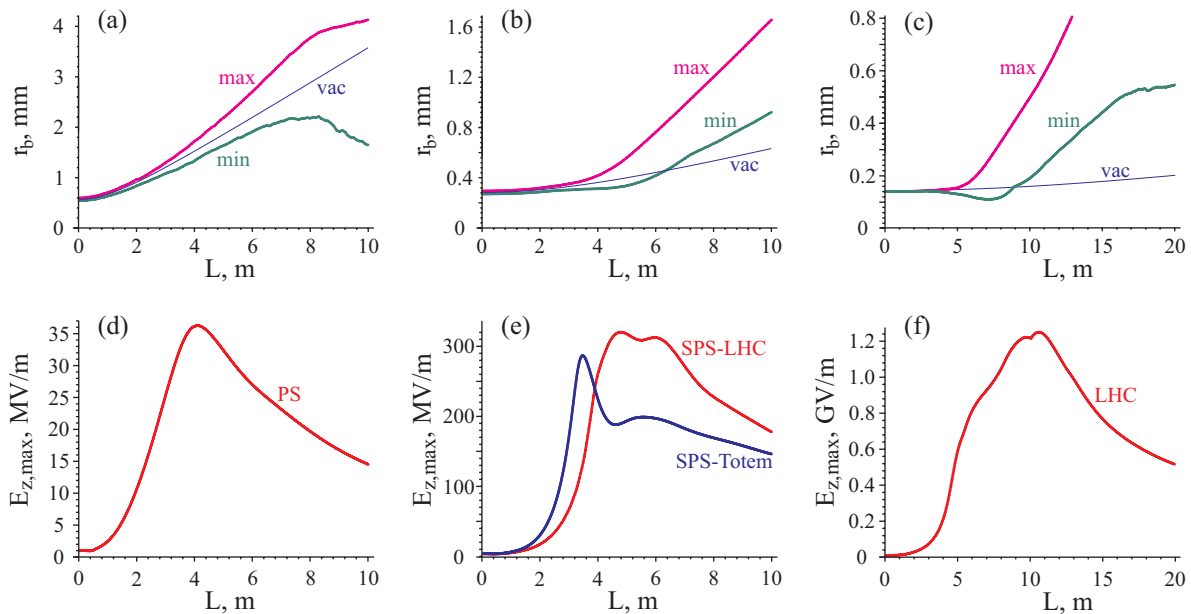


FIG. 2: (Color online) Maximum and minimum rms radius of the proton bunch at longitudinal distances  $\approx \sigma_z$  behind the bunch center (a,b,c) and the maximum wakefield amplitude (d,e,f) versus propagation distance: PS (a,d), SPS-LHC (b,e), SPS-Totem (e), and LHC (c,f). The thin lines in (a,b,c) correspond to free expansion of bunches in vacuum.

the betatron function of accelerator physics. Values of  $L_\theta$  are listed in Table I. The ratio  $L_\theta \omega_b / c$  is greater than 1 for the PS bunch, and smaller than 1 for the SPS bunch, which explains the qualitative difference between the two cases.

There is another effect that could be important for the development of the instability; transverse focusing by plasma fields. To estimate the effect, we compare the energy associated with the transverse motion of protons and the depth of the potential well that focuses the bunch. For long and narrow bunches ( $\sigma_r \lesssim c/\omega_p$ ,  $\sigma_z \gg c/\omega_p$ ) the focusing force is mainly determined by the uncompensated current of the beam. The focusing strength is  $F_r/r \sim 2\pi n_b e^2$ , from which we estimate, for a bunch of radius  $\sigma_r \sim c/\omega_p$ , the depth of the potential well to be

$$W_f \sim \frac{F_r \sigma_r}{2} \sim \frac{m c^2 n_b}{4 n_p}. \quad (6)$$

The energy of transverse motion  $W_{tr}$  is determined by the transverse momentum  $p_{b\perp}$  of bunch particles:

$$W_{tr} = \frac{p_{b\perp}^2}{2\gamma_b M} \approx \frac{\sigma_\theta^2 W_b^2}{2\gamma_b M c^2} = W_b \frac{\sigma_\theta^2}{2} = W_b \frac{\epsilon^2}{2\sigma_r^2}, \quad (7)$$

where  $W_b$  is the incident proton energy. The numerical values are shown in Table II. For the PS bunch, plasma focusing is negligible. For both variants of the SPS bunch, the effect of focusing is visible (some parts of the bunches diverge more slowly than in vacuum), but not strong. For the LHC bunch, the plasma focusing is important and favorable for the instability. The bunch is

pinched by the plasma wave at some cross sections, which results in stronger wakefields. This pinching is visible after 5 – 10 m of propagation in the plasma. At longer distances, the microbunch structure is perturbed by the instability as discussed below.

#### IV. FIELDS FROM MAXIMUM MODULATION

We now suppose we can reach the state where we have maximum modulation of the bunch, and investigate the strength of the electric fields. The bunch has been divided into microbunches which each contains  $\approx 1/2$  of the initial number of protons within one plasma wavelength (the other protons are pushed out by the radial fields). We can use the expression in the first section to estimate the electric field from one microbunch:

$$E_{\mu,z,max} = e N_\mu Z(k_p, \sigma_z) R(k_p \sigma_r) \quad (8)$$

where  $N_\mu$  is the number of protons in the microbunch and  $\sigma_z \approx \sqrt{2} k_p^{-1}$  is the rms length of the protons in the microbunch. If we assume for seeded instabilities that all microbunches behind the center of the proton bunch add coherently to the produced electric field, then we have

$$E_{z,max} \approx \frac{eN}{4} Z(k_p, \sigma_z) R(k_p \sigma_r). \quad (9)$$

We now calculate the maximum electric field by taking  $k_p \sigma_r = 1$ , substituting  $\sigma_z \approx \sqrt{2} k_p^{-1} = \sqrt{2} \sigma_r$ , and using

(2), (3). This yields

$$E_{z,\max} \approx 0.085 \frac{Ne}{\sigma_r^2} \approx 0.12(\text{GV/m}) \cdot \left(\frac{N}{10^{10}}\right) \left(\frac{100 \mu\text{m}}{\sigma_r}\right)^2. \quad (10)$$

The maximum field from this expression is given in Table II. The fields can be compared to the wave-breaking field

$$eE_0 = k_p mc^2$$

to determine the dimensionless field amplitude

$$\alpha = \frac{E_{z,\max}}{E_0} \approx 0.024 \left(\frac{N}{10^{10}}\right) \left(\frac{100 \mu\text{m}}{\sigma_r}\right). \quad (11)$$

As is seen in the table, the values of  $\alpha$  range from 7 % for the SPS-Totem to 25 % for the LHC. Estimate (10) agrees well with simulation results (Fig. 2) for all variants except PS. For the PS bunch, the simulated field is lower because of the angular divergence of the bunch which is not taken into account in (10). As is clear from the formulae in this section, the critical element determining the strength of the wakefields in the modulated bunch case is the transverse density of particles in the drive bunch,  $N/\sigma_r^2$ , so that a reduction of the transverse emittance or an increase in the bunch intensity will have significant effect on the achievable accelerating fields.

## V. EVOLUTION OF THE MICROBUNCHES

There are several effects limiting the distance over which the strong fields act to increase the energy of accelerated particles. If the drive bunch propagates in a uniform density plasma, then the instability destroys the microbunches soon after the maximum field is reached. This effect is clearly seen in Fig. 2 for all four variants. The reason lies in the slow motion of the defocusing field regions with respect to the bunch. This motion continues after the bunch formation is completed and quickly destroys the microbunches [10]. It is possible to avoid the destruction of the microbunch structure by a proper step up in the plasma density (Fig. 3) which modifies the instability growth in such a way that the field motion relative to the bunches stops at the optimal moment [10]. The density step cannot stop the development of the instability immediately. It quickly changes the excited field, but the radially moving protons still have inertia. Thus the density step modifies the instability in such a way that the bunch evolves toward the desired state and the evolution finishes at this state. The values for the parameters  $\delta n_p$ ,  $l_0$ , and  $l_t$  maximizing the established wakefield amplitude are listed in Table III.

The field evolution for the stepped plasma profile is shown in Fig. 4 in comparison with the uniform plasma case. The wakefield is preserved for a long distance, but however has a lower amplitude than in the uniform case. The latter follows from the fact that proton microbunches

TABLE III: Parameters describing the bunch interaction with the plasma in the case of the stepped-up plasma density.

Parameter	PS	SPS-LHC	SPS-Totem	LHC
$\delta n_p$ (%)	2.2	2.4	2	1.6
$l_0$ (m)	1	2.5	1	3
$l_t$ (m)	3	1.5	3	1.5
$N_{mb}$	80	95	130	125
$L_{\text{diff}}$ (m)	130	475	655	2500
$E_{z,\max}$ (MV/m)	13	100	100	900
$L_{\text{depl}}$ (km)	1.8	4.5	4.5	7.8
$W'$	0.00012	0.009	0.004	0.6
$L_{\text{dec}}$ (m)	32	670	470	9500
$W_{\text{dec}}$ (GeV)	0.4	60	40	7700
$W_E$ (GeV)	0.25	10	10	10
$L_{\text{deph}}$ (m)	1.4	250	120	30000
$W_{\text{deph}}$ (GeV)	0.012	16	8	17000

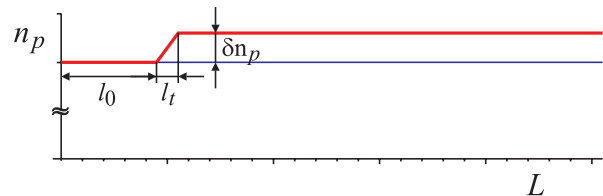


FIG. 3: (Color online) Plasma density profile used in the simulation for the creation of a long-lived train of microbunches.

can create a wakefield over a long distance only if they are located in both the decelerating and the focusing phase of the wakefield, which is only one quarter of the wakefield period. In the uniform plasma, the maximum of the field occurs when the microbunches fill the whole decelerating phase of the wave, which is nearly one half of the period. Thus, the field amplitude for the long-lived microbunch train should be roughly half that of the peak field in the uniform plasma. Simulations confirm this statement for all variants except LHC bunch. For the latter, the field of the long-lived train is substantially increased due to the plasma focusing of the microbunches with respect to their initial size.

While most of microbunches in the long-lived train are well focused by the plasma wave, the head of the first microbunch is not and doubles in size transversely after a distance  $\sim L_\theta$ . Once the first microbunch has diffracted away, the next will start to diffract, and this process is expected to continue until all microbunches are lost. The lower estimate for the scale over which, in the absence of external focusing, the whole bunch diffracts away, is

$$L_{\text{diff}} = N_{mb} L_\theta,$$

where  $N_{mb} \sim \sigma_{z,0}/\lambda_p$  is the number of microbunches. Values of  $N_{mb}$  and  $L_{\text{diff}}$  are given in Table III. However,

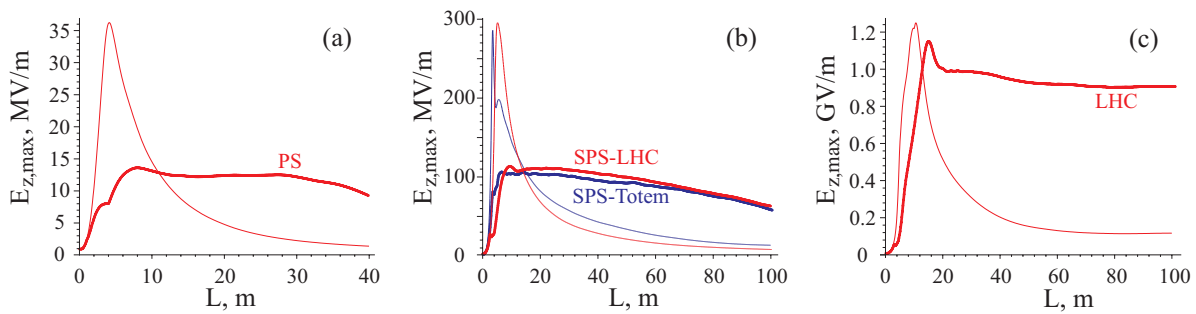


FIG. 4: (Color online) The maximum wakefield amplitude behind the bunch center versus the propagation distance for the stepped-up (thick lines) and uniform (thin lines) plasmas.

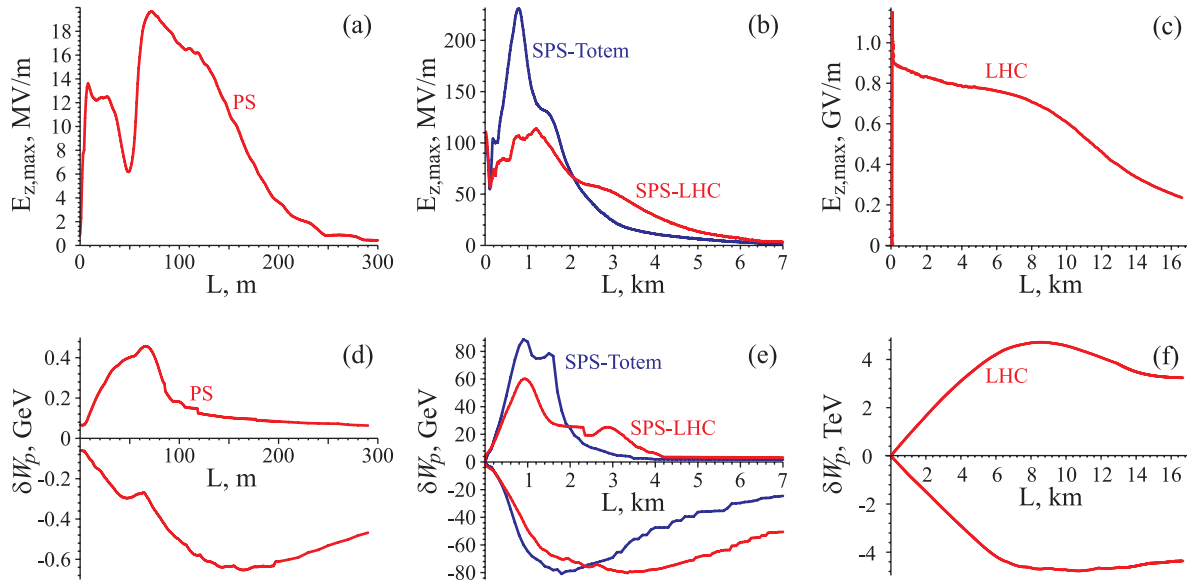


FIG. 5: (Color online) The dependence of the wakefield amplitude (top) and maximum proton energy gain or loss (bottom) over long distances for the stepped-up plasma case.

simulations reveal that the field excitation is preserved over a much longer length [Fig. 5(b,c)] suggesting that only a small fraction of a microbunch becomes unavailable for the wakefield excitation at each path segment of the length  $L_\theta$ .

The second possible limitation on the length of the strong wakefield excitation comes from the energy change of protons in the bunch. The simplest consideration of this effect, estimated by dividing the proton initial energy by the decelerating force,

$$L_{\text{depl}} = \frac{W_P}{eE_{z,\text{max}}}, \quad (12)$$

typically overestimates the length. The distances  $L_{\text{depl}}$  based on simulated values of  $E_{z,\text{max}}$  (Table III) are much longer than the lengths over which the fields decrease in Fig. 5(a,b). A more careful investigation shows that the difference in energy depletion among the protons within a microbunch must be taken into account. For short proton

bunches [2], the energy depletion results in an elongation of the bunch and thereby gradual decrease of the excited wakefield. For trains of microbunches, the mechanism is different, as illustrated by Fig. 6. The microbunches are initially located in such a way with respect to the wakefield that the microbunch head experiences the strongest deceleration. The induced energy chirp along the bunch results in bunch compression and a net shift of the bunch to the point of zero longitudinal field. When this occurs, the bunch stops changing its average energy and contributing to field excitation. When most of the bunches are in this situation, the wakefield drops down, and the bunches get lost transversely since the weaker wakefield cannot keep the protons focused any more.

To estimate the energy change of a microbunch with distance, we assume a constant wave amplitude and consider the process in the reference frame moving with the phase speed of the wave  $V \approx c$ . The wakefield  $E'_z$  and



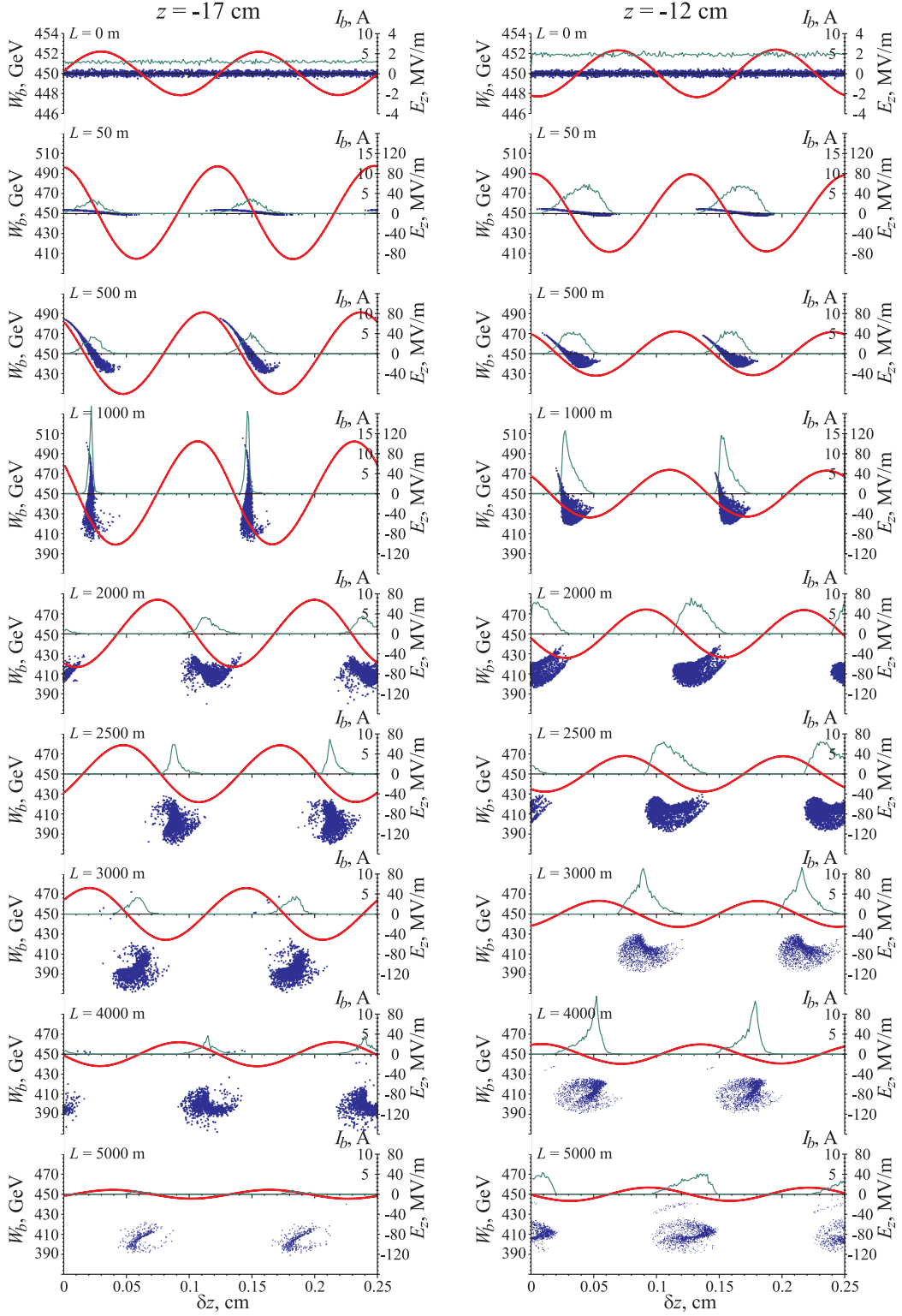


FIG. 6: (Color online) Evolution of several SPS-LHC microbunches: energy  $W_b$  of bunch particles (dots), on-axis electric field  $E_z$  (red line), and bunch current  $I_b$  through the circle of radius  $c/\omega_p$  (green line) vs longitudinal coordinate  $\delta z$  at various distances traveled in the stepped-up plasma. The coordinates  $\delta z$  are measured from points moving with the speed of a 450 GeV proton and initially located 17 cm (left column) or 12 cm (right column) behind the bunch center.

the on-axis potential  $\Phi'$  in this frame are

$$E'_z = -E_{z,m} \sin k'_p z', \quad \Phi' = -\frac{eE_{z,m}}{k'_p} \cos k'_p z', \quad (13)$$

where  $E_{z,m}$  is the on-axis field amplitude in the labora-

tory frame,  $k'_p = \omega_p/(\Gamma V)$  is the wavenumber in the moving frame,  $\Gamma = (1 - V^2/c^2)^{-1/2}$ , and the coordinate  $z'$  is measured from a zero field point. In the potential well (13), a proton starting from the point of the strongest field ( $k'_p z' = \pi/2$ ) gains a maximum kinetic energy (in units of the rest energy) of

$$W' = \frac{eE_{z,m}}{k'_p M c^2}. \quad (14)$$

Values of  $W'$  for  $E_{z,m} = E_{z,\max}$  are listed in Table III. For the first three variants,  $W' \ll 1$ , and the motion of bunch particles in the moving frame is not relativistic. The frequency of particle oscillations near the bottom of the potential well is thus independent on the amplitude and equals

$$\omega_{z'} = \sqrt{\frac{eE_{z,m}k'_p}{M}}. \quad (15)$$

Simultaneous events separated in the laboratory frame by the distance  $c/\omega_p$  (i.e., by the microbunch length) differ in the moving frame by the time interval  $(k'_p c)^{-1} = \sqrt{W'}/\omega_{z'}$ . For  $W' \ll 1$ , we can neglect this time difference and consider the bunch particles to start their motion simultaneously in the moving frame. Consequently, after the time  $\pi/(2\omega_{z'})$  in the moving frame and the distance

$$L_{\text{dec}} = \frac{\pi c \Gamma}{2\omega_{z'}} \approx \frac{\pi c \Gamma^{3/2}}{2\omega_p} \sqrt{\frac{M E_0}{m E_{z,m}}} \quad (16)$$

in the laboratory frame, a considerable fraction of the protons collect at the bottom of the potential well (Fig. 6,  $L = 1000$  m). This is the typical length scale over which the microbunch gives up the energy to the wave, if the bunch was initially located in the decelerating phase of the wakefield. To obtain the energy scale, we Lorentz transform the energy (14) and the corresponding momentum to yield the energy loss of protons

$$W_{\text{dec}} = W_P \sqrt{2W'}. \quad (17)$$

For the LHC bunch ( $W' = 0.6$ ), the above formulae are marginally correct, but still can be used as order-of-magnitude estimates. Values of  $L_{\text{dec}}$  and  $W_{\text{dec}}$  are given in Table III. For the LHC case,  $W_{\text{dec}} > W_P$ , implying that the longitudinal shift of depleted particles is not a limiting factor.

The real picture of wave-microbunch interactions is more complicated than that described in our simplified model, as can be seen in Fig. 6. Since the wave is created by the microbunches themselves, the cross-section of zero  $E_z$  moves backward together with upstream microbunches, and compressed microbunches are formed in a decelerating field rather than at the point of zero acceleration. As a consequence, the distance of strong field excitation is longer than  $L_{\text{dec}}$  (Fig. 5, top), the energy loss of protons is greater than  $W_{\text{dec}}$  (Fig. 5, bottom),

and protons do not make a full circle on the longitudinal phase plane taking the energy back from the wave, but instead stick to the zero-field point and stop energy exchange with the wave (Fig. 6).

## VI. ELECTRON ENERGY GAIN

If test electrons of energy  $W_E \gg mc^2$  are injected into the wakefield, their energy gain (Fig. 7) is much lower than the energy gain of the most energetic protons for all variants except the LHC [Fig. 5(d-f)]. The reason is the dephasing between electrons and the wakefield. The typical distance at which a fast electron outruns a proton with the relativistic factor  $\Gamma$  by the half of the wakefield period (and crosses the whole acceleration phase of the wave) is

$$L_{\text{deph}} = 2\pi\Gamma^2 c/\omega_p. \quad (18)$$

To obtain the typical energy gain we multiply this distance by the average accelerating field:

$$W_{\text{deph}} = \frac{2}{\pi} e E_{z,\max} L_{\text{deph}}. \quad (19)$$

The resulting values are given in Table III. The parameters obtained in simulations are close to (18)–(19). For the PS case, electrons were injected into the wakefield several times at various stages of bunching [Fig. 7(a)], but for all groups the maximum electron energy is the same.

To obtain higher energy electrons from the PS or SPS energy proton bunches, it would be necessary to achieve larger gradients. This would require larger drive bunch density, either through lower emittances or larger numbers of drive particles.

## VII. LIMITATIONS DUE TO INTERACTIONS

As discussed in [1], proton interactions in the plasma are not a limiting factor. For typical values of  $n_p$  in the range  $10^{14} - 10^{16} \text{ cm}^{-3}$ , the mean-free-path for inelastic reactions of high energy protons with the plasma are orders of magnitude larger than the simulated plasma cell lengths. The transverse growth rate of the proton bunch due to multiple scattering is also very small compared to other effects discussed here. For electrons, the radiation lengths for the plasma densities of interest here are also very long compared to the lengths of the plasma cells under consideration, so that particle interactions in the plasma are not expected to be a limiting factor.

## VIII. SUMMARY

We have investigated the wakefield amplitudes which could be achieved via the modulations of a long proton



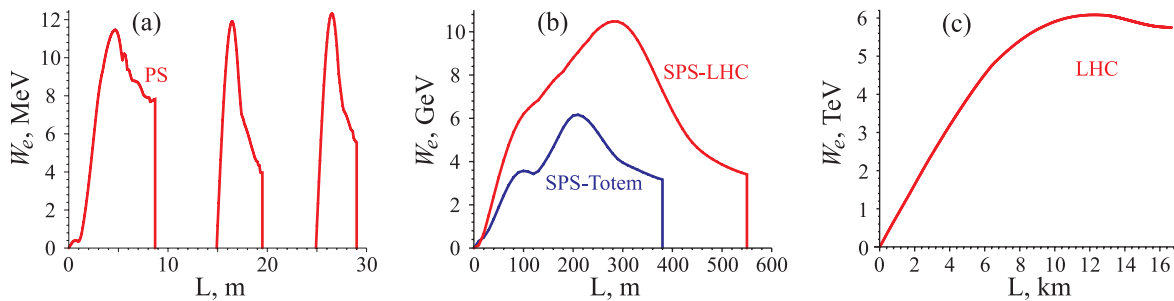


FIG. 7: (Color online) The maximum energy gain of electrons versus propagation distance for the stepped-up plasma case.

bunch. The key result in the parametric investigation is that, in the limit of long bunches compared to the plasma wavelength, the strength of the accelerating fields is directly proportional to the transverse particle density in the drive bunch,  $N/\sigma_r^2$ . This finding puts a premium on increasing this quantity for beams designed specifically for beam driven wakefield acceleration via the modulation technique.

The scaling laws were tested and verified in detailed simulations using parameter sets for existing or planned proton bunches at CERN; i.e., PS, SPS and LHC bunch parameters. For existing bunch parameters, it was found that electric fields of about 35, 300, 1200 MeV/m should be achievable for the PS, SPS and LHC bunches, respectively. These gradients cannot be maintained over arbitrarily long distances because the modulation process will eventually destroy also the microbunch structure. To overcome this deleterious effect, it has been shown that a density step in the plasma can freeze the microbunch structure, albeit at a penalty in the maximum achievable gradients.

A detailed investigation of the evolution of the microbunches was undertaken for the stepped-up plasma

density scenario. It was found that significant accelerating gradients could be maintained over long distances, although the resulting energy gains for electrons were moderate due to dephasing effects for the PS and SPS cases. For the LHC, the protons are relativistic enough that dephasing is not a significant issue, and in this case test electrons were accelerated beyond 6 TeV with gradients approaching 1 GeV/m. It is anticipated that the achieved energy gains could be substantially more favorable if the transverse density of protons could be improved for all scenarios considered.

## IX. ACKNOWLEDGEMENTS

The authors are grateful to C. Huang, A. Pukhov, O. Reimann, J. Viera and G. Xia for stimulating discussions. Different parts of this work are supported by RFBR Grants 09-02-00594, 11-01-00249, 11-02-00563, 11-02-91330, and by the Russian Ministry of Education grants 2.1.1/3983 and 14.740.11.0053.

- 
- [1] A. Caldwell, K. Lotov, A. Pukhov, and F. Simon, *Proton Driven Plasma Wakefield Acceleration*, Nature Phys., **5**, 363 (2009).
  - [2] K.V.Lotov, *Simulation of proton driven plasma wakefield acceleration*, Phys. Rev. ST - Accel. Beams, **13**, 041301 (2010).
  - [3] G. Xia, A. Caldwell, K. Lotov, A. Pukhov, R. Assmann, F. Zimmermann, *A Proposed Experiment on the Proton Driven Plasma Wakefield Acceleration*, Proc. 1st International Particle Accelerator Conference 2010 (Kyoto, Japan), p.4392-4394.
  - [4] G. Xia et al., *Update of Proton Driven Plasma Wakefield Acceleration*, In: Advanced Accelerator Concepts, 14th Workshop, AIP Conference Proceedings, edited by S.H.Gold and G.S.Nusinovich, v.1229, p.510-515 (AIP, 2010).
  - [5] N. Kumar, A. Pukhov, K. Lotov, *Self-modulation instability of a long proton bunch in plasmas*, Phys. Rev. Lett. **104**, 255003 (2010).
  - [6] W. Lu, C. Huang, M. M. Zhou, W. B. Mori and T. Katsouleas, *Limits of linear plasma wakefield theory for electron or positron beams*, Phys. Plasmas **12**, 063101 (2005).
  - [7] C. Joshi (private communications).
  - [8] K.V.Lotov, *Simulation of ultrarelativistic beam dynamics in plasma wake-field accelerator*, Phys. Plasmas, **5**, 785 (1998).
  - [9] K.V.Lotov, *Fine wakefield structure in the blowout regime of plasma wakefield accelerators*, Phys. Rev. ST - Accel. Beams, **6**, 061301 (2003).
  - [10] K.V.Lotov, *Controlled self-modulation of high energy beams in a plasma*, Phys. Plasmas, **18**, 024501 (2011).